Electronic Supplementary Material (ESI) for Inorganic Chemistry Frontiers.

Supporting Information

Using Dual Site-Substitution Strategy to Inhibit Staircase-like Electrochemical Profiles for High-performance Na-ion Battery Cathode

Kun Luo*, Wenhui Li, Yang Jiang, Houze Song

School of Materials Science and Engineering, Tianjin University of Technology, Tianjin, 300384, PR China

Corresponding author: Email: kunluo@email.tjut.edu.cn

Experimental

Material synthesis. $Na_{2/3}MnO_2$ and $K_{0.05}Na_{0.62}Mn_{0.9}Ti_{0.1}O_2$ samples were synthesized by mixing Na_2CO_3 (Aladdin, anhydrous 99.8 %), K_2CO_3 (Aladdin, anhydrous 99 %), MnO_2 (Aladdin, 99 %) and TiO_2 (Macklin, 99.8 %) in a stoichiometric amount and the mixture was then pelletized and heated up to 1050 °C with a heating rate of 1 °C min^{-1} under atmospheric conditions for 10 hours. Once synthesized the samples were transferred to an Ar-filled glove box in order to avoid the contact with the atmosphere.

Structural characterization. Power X-ray diffraction (PXRD) patterns were collected using a powder X-ray diffraction (XRD) meter (Smart Lab 9 KW) with Cu Kα radiation. Environment scanning electron microscope images were carried out to determine the morphology and composition contents of the materials on Quanta FEG 250. High-resolution transmission electron microscopy (HRTEM) and element analysis were conducted on a FEI Tecnai G2F 20. X-ray photoelectron spectroscopy spectra (XPS) conducted by XPS microprobe (ESCALAB250Xi) with an Al Kα X-ray source (1486.6 eV) was used to study the surface chemical composition and valence state of the elements of the samples. Raman spectroscopy was performed using a HORIBA EVOLUTION Microscope with 532 nm excitation laser wavelength. Fourier-transform infrared spectroscopy (FTIR) spectroscopy for the electrolyte structure is conducted on Frontier Mid-IR FTIR/STA6000-TL9000-Clarus SQ8. Nuclear magnetic resonance (NMR) is characterized on AVANCE III HD 400M HZ.

Electrochemical Measurements. The electrodes are composed of active materials, Super-P and polyvinylidene fluoride (PVDF) in a weight ratio of 8:1:1. The electrode loading of active material is about 3-5 mg/cm^2. The obtained slurry was applied on Al foil and dried at 80 °C overnight under vacuum before use. Electrochemical cell tests

were conducted after assembling a R2032 coin-type cell using sodium metal as the anode in an Ar-filled glove box. The electrolyte solution consisted of 1 M $NaClO_4$ in propylene carbonate (PC). The galvanostatic charge/discharge measurement was performed in the potential range from 1.5 - 4.3 V with a multichannel battery testing system.

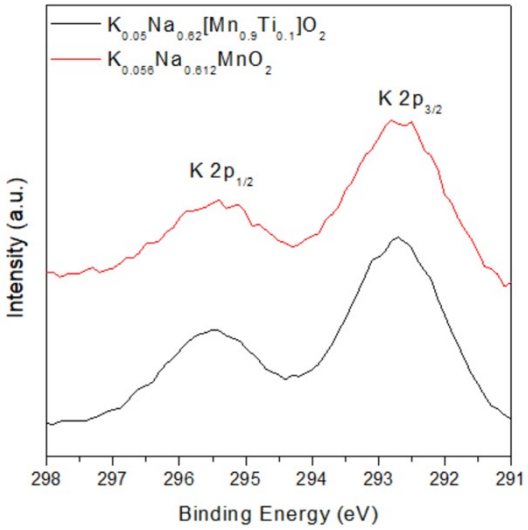

Figure S1 XPS profiles of the reference material $Na_{0.612}K_{0.056}MnO_2$ and the modified $Na_{0.62}K_{0.05}Mn_{0.9}Ti_{0.1}O_2$.

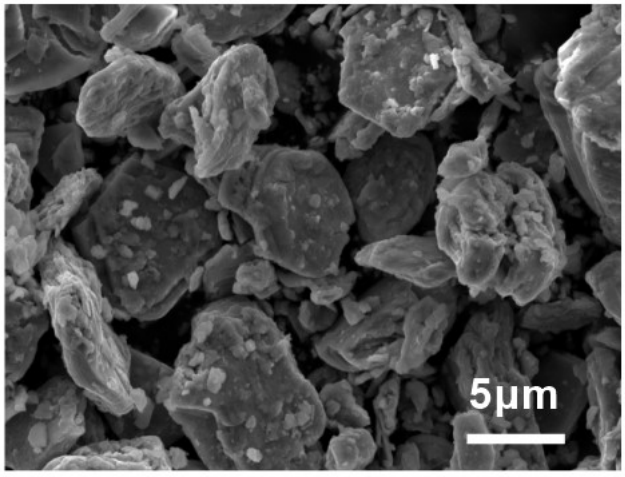

Figure S2. SEM image of NMO.

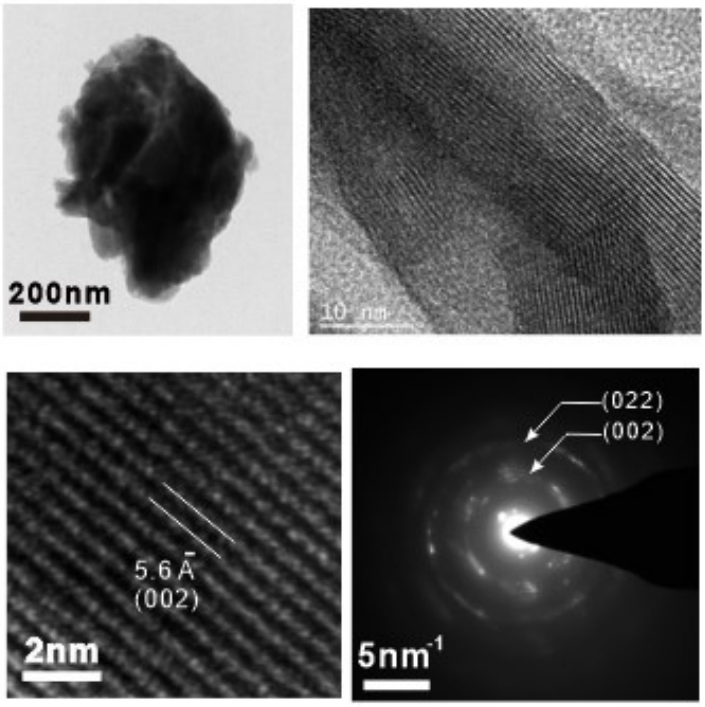

Figure S3. TEM images of NMO.

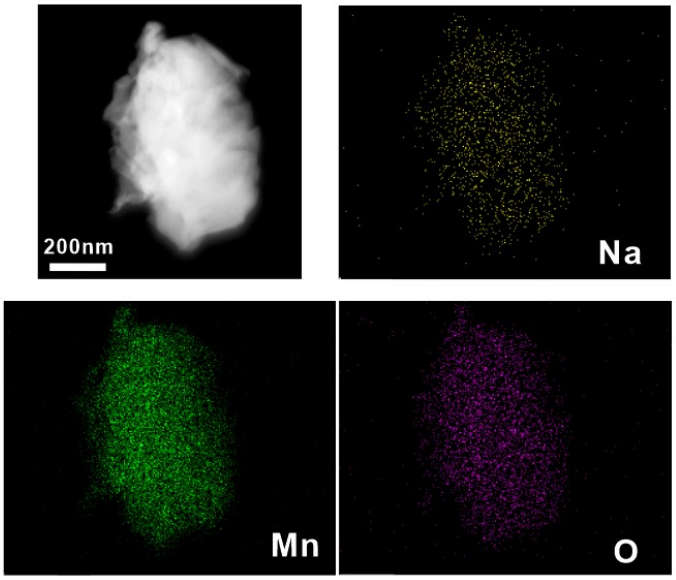

Figure S4. EDS mapping of NMO

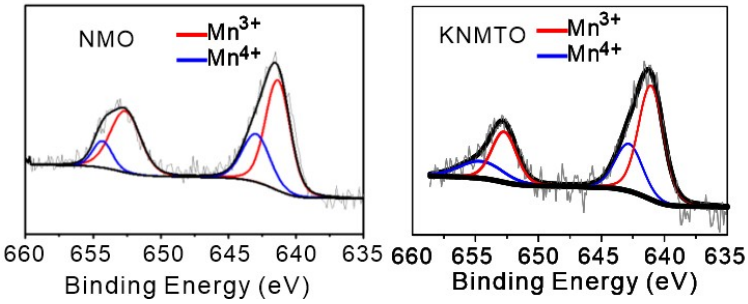

Figure S5 XPS profiles of NMO and KNMTO samples

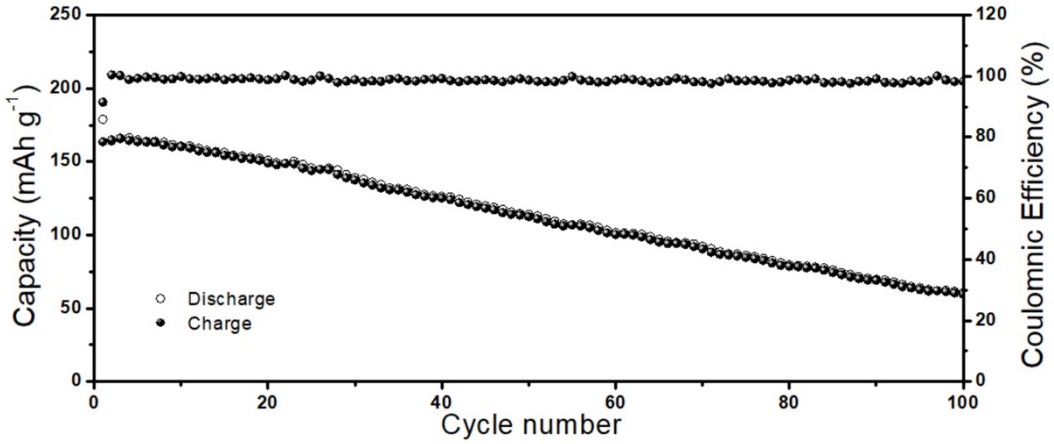

Figure S6. Cycling performance of NMO at charge/discharge rate of 50 mA g^{-1}.

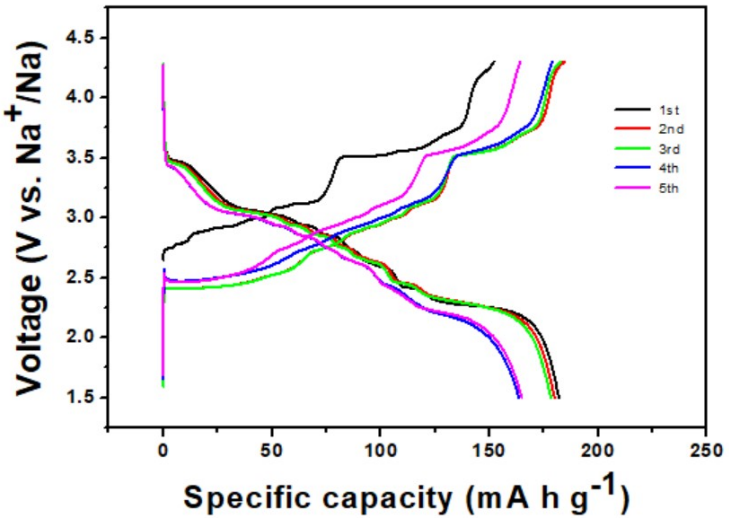

Figure S7 Charge/discharge curves of NMO for the first five cycles at 50 mA g^{-1}.

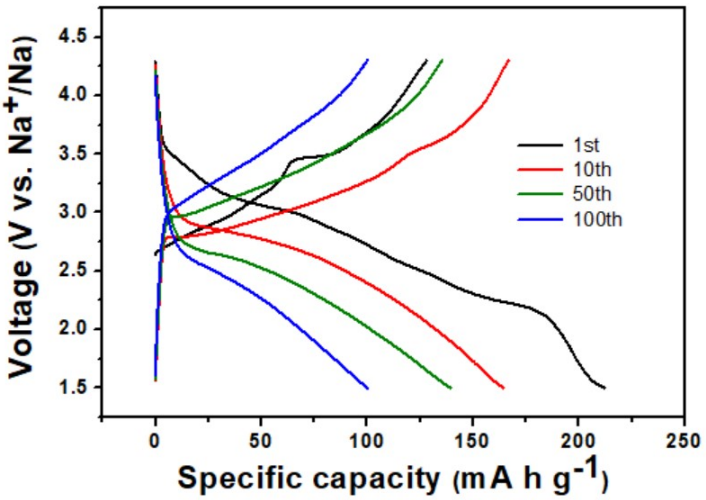

Figure S8 Charge/discharge curves of NMO for various cycles at 50 mA g^{-1}.

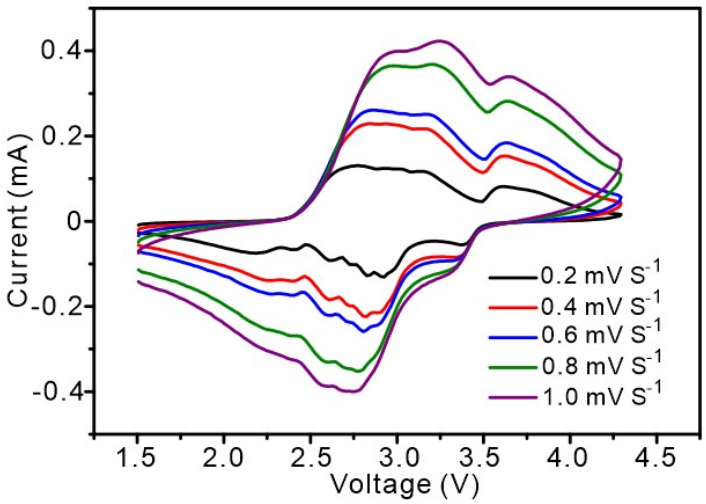

Figure S9. CV curves of NMO at various scan rates.

The Na^+ diffusion coefficient can be determined from the CV results as shown in the figures below by the linear relationship between redox peak current and the square root of scan rate, which can be calculated with the following equation:

$$i_p = \left(2.69\times10^5\right)\times n^{3/2} A D_{Na^+}^{1/2} v^{1/2} C_{Na^+}$$

Where n and C_{Na+} are the charge transfer and concentration of Na^+, A is the area of electrode. The higher fitted slope of i_p vs. $v^{1/2}$ indicates higher Na^+ diffusion coefficient. The D_{Na+} value of the KNMTO material calculated is approximately 10^{-10}-10^{-9} cm^2 s^{-1}, which is consistent with the value obtained from GITT results.

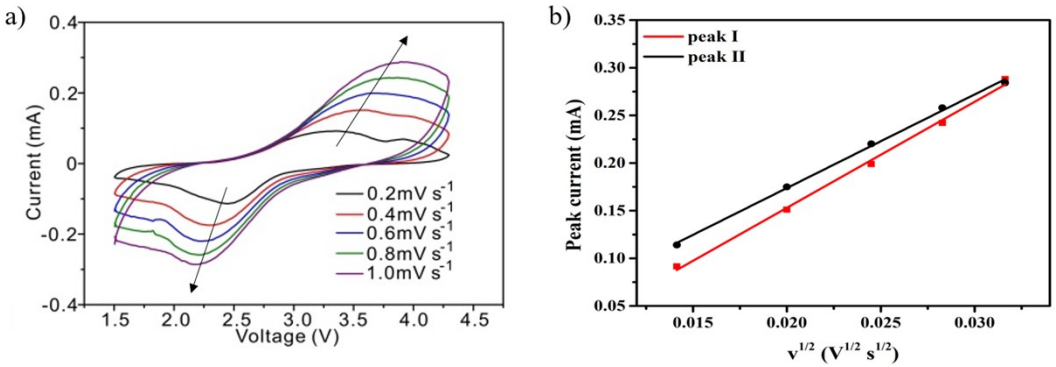

Figure S10 a) CV curves at different scan rates. b) i versus log(v) plots at specific peak currents.

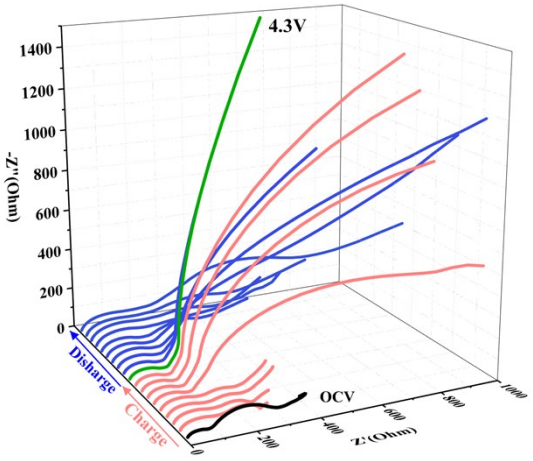

Figure S11 In-situ EIS tested between 1.5-4.3 V during charge and discharge process.

Ex-situ electrochemical impedance spectrometry (EIS) data of the cathode material is carried out at different electrochemical stages in order to study the changes of resistance during the charge/discharge processes. The mid-frequency semicircle and high-frequency semicircle correspond to the interphase charge transfer impedance (R_{CT}) and resistance of the solid electrolyte interphase (SEI) layer (R_{SEI}), respectively. (*Adv. Energy Mater. 2018, 8, 1801441; Chem. Eng. J. 2023, 8, 475*) The R_{SEI} achieves the minimum value (62 Ω) during the initial charge process and then increases gradually as the voltage increases, indicating that the SEI layer is formed. (*Carbon Energy 2022, 5, e191*) After charged up to 3.5 V, there is only a semi-circle, which is caused by the decomposition of the SEI film at high voltage. (*Nat. Energy 2022, 7, 718-725*)

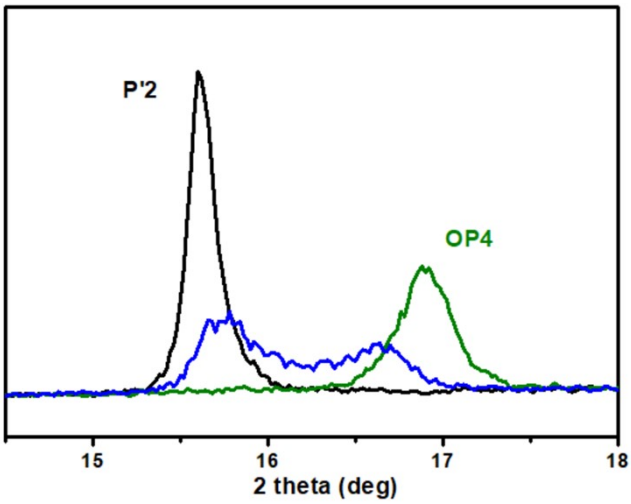

Figure S12. XRD patterns of the (002) peak of pure P’2 and OP4 phases.

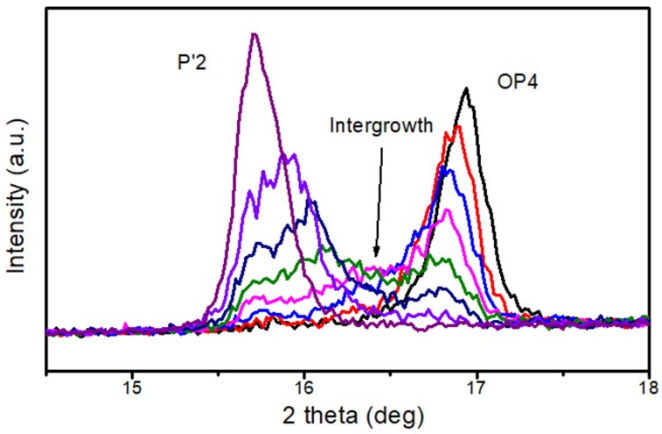

Figure S13. Evolution of (002) peak for phase transition in the discharge process.

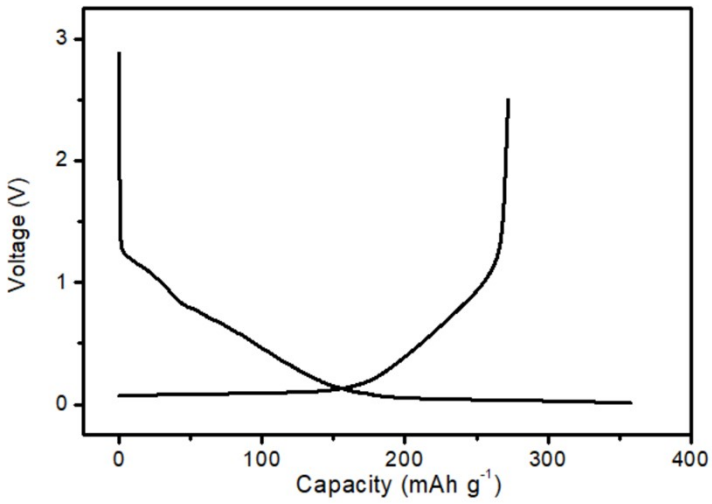

Figure S14. Charge/discharge curves of hard carbon.

Table S1. Crystallographic and Rietveld refinement data of P2'-type NMO cathode.

Space group: *Cmcm* (63) a = 2.834(1) Å, b = 5.255(5) Å, c = 11.211(2) Å, Volume: 166.96 (1) Å^3

Atom	Site	x	y	z	Occupancy
Na1	4c	0	-0.068(2)	0.25	0.241(6)
Na2	4c	0	0.312(4)	0.25	0.429(6)
Mn	4a	0	0	0	1
O	6c	0	0.648(8)	0.093(4)	1

Table S2. Crystallographic and Rietveld refinement data of P2'-type KNMTO cathode.

Space group: *Cmcm* (63) a = 2.842(1) Å, b = 5.269(4) Å, c = 11.226(2) Å, Volume: 168.103(7) Å^3

Atom	Site	x	y	z	Occupancy
Na1	4c	0	-0.049(3)	0.25	0.174(8)
Na2	4c	0	0.327(2)	0.25	0.446(8)
K	4c	0	-0.049(3)	0.25	0.050(8)
Mn	4a	0	0	0	0.9
Ti	4a	0	0	0	0.1
O	6c	0	0.664(9)	0.083(4)	1